Spatial Ambient Noise Inversion Using a Single Hydrophone

Ahmed Mahmood, Mandar Chitre and Hari Vishnu
Acoustic Research Laboratory, Tropical Marine Science Institute, National University of Singapore
e-mail: {ahmed, mandar, hari}@arl.nus.edu.sg

***Abstract*—We formulate a new approach to extract environmental information from a *single* omnidirectional hydrophone receiver that passively senses ambient noise. Recorded samples essentially hold information about the ocean itself as the pressure waveforms at the noise source and receiver are different due to distortions induced by the underwater acoustic channel. Our scenario of interest is warm shallow waters, where the ambient soundscape is dominated by snapping shrimp noise at medium-to-high frequencies. By taking only the direct arrival and surface reflection into account, we show that the hydrophone's depth can be deduced *passively* by using an autocorrelation function (ACF) derived from the ambient noise process. Moreover, the ACF can be exploited further to derive the snap distribution as a function of range from the hydrophone receiver, which in turn offers key advantages in environmental monitoring of warm shallow waters.**

I. Introduction

Ocean noise depends largely on local conditions and varies considerably in different scenarios. For example, in shallow tropical waters, the sea floor is typically colonized by the snapping shrimp [1]–[3]. The ambient noise in such environments is impulsive and also exhibits memory [1], [4]. In fact, snapping shrimp noise dominates the acoustic spectrum at frequencies greater than 2 kHz [5]. The work presented in this manuscript focuses on underwater channels dominated by such noise.

Though researchers have tried to model the snapping shrimp noise process [4], [6], much is still unknown about it. For example, little is known about the effective spatial distribution of snaps. While local spatial distributions can be mapped, this requires high-frequency hydrophone arrays [2], [7]. This in turn offers substantial benefits in applications such as rapid environment assessment, environmental monitoring [8], etc. Moreover, such distributions can help researchers develop much needed forward models that characterize the noise dependency within hydrophone arrays. Recent works in underwater acoustic communication have highlighted significant returns in employing algorithms that exploit amplitude statistics as well as memory within snapping shrimp noise [9], [10]. Similarly, by invoking appropriate spatial noise models, one can design algorithms that take the mutual information of the noise amongst the sensors into consideration to achieve superior performance.

Passive sensing using snapping shrimp noise is not a new problem. Various works, such as [3], highlight the potential of detecting submerged objects by taking the geometry of the channel into account. Moreover, several researchers have proposed algorithms that localize individual snaps (range and bearing) using channel geometry or sparsity methods [11], [12]. Though such approaches offer an estimate of a spatial snap distribution, this requires a multitude of expensive sensors. Further still, the problem becomes increasingly computationally demanding as the number of sensors increases.

Our contributions are as follows: We explore the amount of information one can exploit from a single omnidirectional hydrophone by passively sensing snapping shrimp noise. The primary question addressed is, what information of a snapping shrimp populace can be determined from noise observed at a single hydrophone? Though spatial arrays have offered results in the past, the problem we put forth is that of doing it with a minimalistic setup, i.e., a *single* immersed hydrophone. By considering the channel geometry, an omnidirectional hydrophone can potentially allow us to evaluate snapping shrimp densities as a function of range (from the hydrophone). The question posed above is essentially an inverse problem for which a forward model needs to be developed. Our approach is to initially convert the received observations to impulsive event arrivals (IEAs). The latter is essentially a realization of a point process in time [1], [4]. We therefore build a forward model for IEAs rather than actual noise observations. This allows us to deal with a process that encapsulates temporal statistics of 'significant' snaps, while doing away with impulsive fluctuations within snapping shrimp noise. Our results conclude that the spatial snap density can indeed be evaluated from the autocorrelation function (ACF) of the IEAs. We are also able to discern other features, such as the receiver operation depth and average snap duration.

This paper is organized as follows: We briefly comment on snapping shrimp noise, IEAs and their respective ACFs in Section II. We derive the two-ray forward model for the ACF of an IEA process in Section III. This is followed by a discussion on the corresponding inversion in Section IV. We finally wrap up by presenting our conclusions in Section V.

II. Snapping Shrimp Noise

Snapping shrimp noise is known to be impulsive and exhibits memory [1]. This results in outliers clustering together thus creating bursty impulsive noise. Denoting a realization of snapping shrimp noise by $w(t)$, where t is the continuous time index measured in milliseconds (ms), we present one such realization in Fig. 1. The data was sampled at 180 kHz and was recorded off the coast of Singapore. One can clearly observe the impulsive characteristics and memory within the realization. The noise samples can be converted to IEAs by

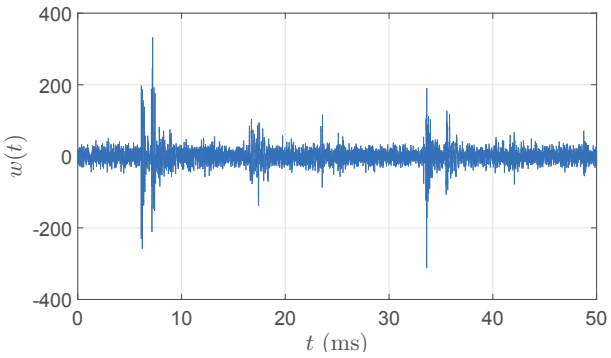

Fig. 1. A realization of snapping shrimp noise.

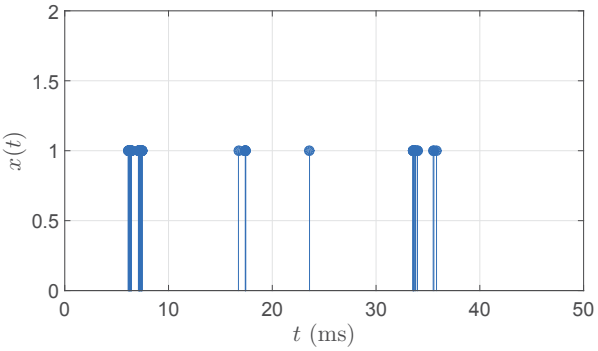

Fig. 2. Snapping shrimp noise after thresholding.

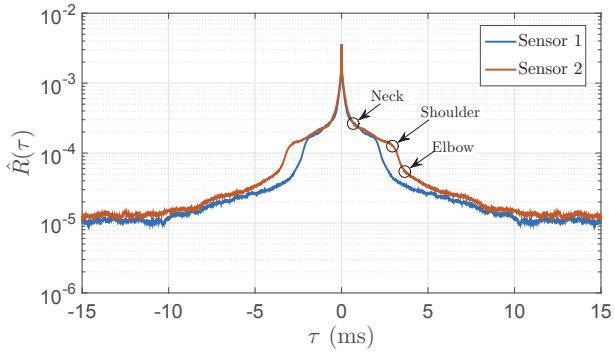

Fig. 3. Average sample ACFs of $x(t)$ obtained from two hydrophones at different depths.

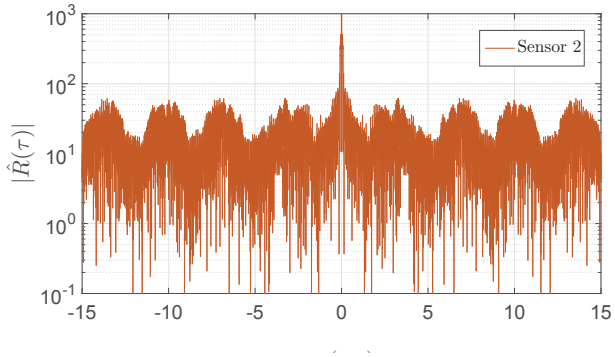

Fig. 4. Average sample ACFs of $w(t)$.

mapping those that exceed a certain absolute threshold to one and setting all remaining to zero. Mathematically, the IEAs are determined by

$$x(t) = \begin{cases} 1 & \text{if } |w(t)| > \epsilon \\ 0 & \text{otherwise,} \end{cases} \tag{1}$$

where ϵ is a predetermined event (impulse) detection threshold which can be evaluated in accordance to the rules laid down in [1], [4]. In our work, we employ $\epsilon = 20\hat{\delta}$, where $\hat{\delta}$ is the scale estimated from $x(t)$ under the assumption that the latter's amplitude distribution is symmetric α-stable (SαS) [4], [6]. We employ the maximum-likelihood estimate for scale [13]. Note that $x(t)$ is a realization of a point process and $x(t) = 1$ signifies an *impulsive event* on the time axis.

Now that we have defined $x(t)$, we present in Fig. 3 the *average* sample ACFs of $x(t)$ observed from two sensors (of the same make) deployed simultaneously at *different* depths at the same geographic location. The curves were evaluated by averaging 250 sample ACFs, each computed from 10^6 sample-long blocks (~ 5.56 s). We note that the employed block length is small enough to assume wide-sense stationarity (WSS) of the process [1]. Moreover, the averaging is necessary as the noise is non-stationary and our approach requires the average noise statistics to deduce snap density [1], [4]. Mathematically, let T be the duration used to compute each ACF block, f_s the employed sampling frequency and $x(t)$ be non-zero within $t \in [0, T)$. Then the *unbiased* sample ACF for the i^{th} block is computed as

$$\hat{R}_i(\tau) = \frac{1}{T-\tau}\int_0^T x(t)x(t+\tau)\mathrm{d}t,$$
$$\Rightarrow \hat{R}_i[k] \approx \frac{1}{N-k}\sum_{n=0}^{N-1} x[n]x[n-k], \tag{2}$$

where $T = N/f_s$, $N \in \mathbb{Z}^+$ and square brackets denote discretized signals, i.e., $x(n/f_s) = x[n]$ and $\hat{R}_i(k/f_s) = \hat{R}_i[k]$. The block ACFs are then averaged out to get $\hat{R}[k]$.

The ACFs in Fig. 3 depict some interesting characteristics. For starters, they each consist of three sharp bends within the curve, which we label as the neck, shoulder and elbow. These have been highlighted for the $\hat{R}(\tau)$ corresponding to sensor 2. The naming convention stems from the ACFs' similarity with the outline of the human form. We note that both curves exhibit a certain structure up until 10 ms, after which the noise floor becomes dominant. As the only difference in the sensors are their respective depths, with sensor 2 being deeper, it can be fairly deduced that the elongated shoulder of sensor 2's ACF is a consequence of increased depth. Therefore, one can potentially evaluate the depth of the hydrophone by *just* passively listening to the ambient noise and invoking no measurements from depth sensors whatsoever. Later on in Section III, we show that the characteristics in Fig. 3 can be sufficiently defined by employing a two-ray model consisting of direct arrivals (DAs) and/or surface reflections (SRs). In fact, each bend in the ACF can be explained in terms of

deployment parameters and/or environmental attributes of the ocean.

On another note, we see that though the sample ACF of $w(t)$ can be computed, this does not average out into the smooth curves presented in Fig. 3. This is due to the fact that snapping shrimp noise is impulsive and its tail characteristics are modeled extremely well by non-Gaussian symmetric α-stable (SαS) distributions, which in turn have non-existent second order moments [9], [14], [15]. To highlight this, we plot the $|\hat{R}(\tau)|$ of $w(t)$ for sensor 2 in Fig. 4. Clearly, the structure in Fig. 4 is not as visible here. The purpose of investigating $x(t)$ instead of $w(t)$ is to do away with the amplitude distribution of the snaps and deal only with the temporal structure within. Moreover, using properties of the point process, one can express the model's ACF in a simplified form. This, in turn, allows one to formulate the inverse problem in a relatively straightforward manner.

III. The Forward Model

Let $X(t)$ denote the stochastic process whose realization is $x(t)$. Then as $X(t) \in \{0, 1\}$, its ACF is given by

$$\begin{aligned} R(\tau) &= E[X(t)X(t+\tau)], \\ &= \mathrm{P}[X(t) = 1, X(t+\tau) = 1], \end{aligned} \tag{3}$$

where $E[\cdot]$ is the expectation operator. Note that we consider $X(t)$ to be WSS as $R(\tau)$ models the long-term sample average $\hat{R}(\tau)$. We can express (3) further as

$$R(\tau) = \mathrm{P}[X(\tau) = 1 | X(0) = 1]p, \tag{4}$$

where $\mathrm{P}[X(t) = 1] = p$. From (4), we immediately deduce that $R(0) = p$ and $R(\tau) \to p^2$ as $\tau \to \infty$. Moreover, as $R(\tau) = R(-\tau)$, we consider $\tau \in \mathbb{R}_{\geq 0}$ in our approach as this can be trivially extended to $\tau \in \mathbb{R}_{<0}$ by replacing τ with $|\tau|$.

We consider a two-ray (DA-SR) model and the following simplifications:

- At any given time, the probability of receiving two or more arrivals is negligibly small.
- As the water surface is essentially an acoustic mirror, for every DA, there is a SR that accompanies it.
- Snaps that come from afar will result in an overlapping DA-SR pair. However, due to the attenuation of sound in seawater, the received pressure waveforms are weak and do not trigger an IEA. Thus the DA-SR pair are considered to have non-overlapping arrivals, with the SR always arriving later.
- There is no chorusing within the snapping shrimp populace. This implies that the snaps occur independently from one another, both in space and time.
- A flat-bottom is considered and snaps are assumed to originate from the sea floor.

As highlighted in [5], [7], snapping shrimp do indeed chorus. Thus snaps are correlated in time and may originate within spatially distributed clusters on (or above) the sea floor. Moreover, the flat-bottom assumption rarely holds in reality. Though our assumptions are simplistic, the definitions and mathematical steps adopted in our approach may be extended to the case that consider a general bathymetry and/or arbitrary snap locations. We comment on how these assumptions impact our model as we derive the latter.

The aforementioned properties result in the equality

$$\mathrm{P}[X(t) = \ell_1] = \mathrm{P}[X(t) = \ell_2] = p/2, \tag{5}$$

where $X(t) = \ell_1$ and $X(t) = \ell_2$ implies $X(t) = 1$ due to a DA and SR in a DA-SR pair, respectively. Moreover, as ℓ_1 and ℓ_2 are essentially disjoint sets, then from (3) and (5), we finally have

$$\begin{aligned} R(\tau) &= \frac{p}{2} \sum_{i=1}^{2} \sum_{j=1}^{4} \mathrm{P}[X(\tau) = \ell_i | X(0) = \ell_j], \\ &= p^2 + \frac{p}{2} \sum_{i=1}^{2} \sum_{j=1}^{2} \mathrm{P}[X(\tau) = \ell_i | X(0) = \ell_j], \end{aligned} \tag{6}$$

where ℓ_3 and ℓ_4 also signify a DA and SR from a DA-SR pair, respectively, but originate from a different source than the one corresponding to ℓ_1 and ℓ_2. As our model does not consider chorusing, the events $X(\tau) = \ell_3$ and $X(\tau) = \ell_4$ are independent of $X(0) = \ell_1$ and $X(0) = \ell_2$. Further still, as $\mathrm{P}[X(\tau) = \ell_1 | X(0) = \ell_1] = \mathrm{P}[X(\tau) = \ell_2 | X(0) = \ell_2]$ and a SR always arrives later than the DA, (6) simplifies to

$$\begin{aligned} R(\tau) = p^2 + p\mathrm{P}[X(\tau) = \ell_1 | X(0) = \ell_1] \\ + \frac{p}{2}\mathrm{P}[X(\tau) = \ell_2 | X(0) = \ell_1]. \end{aligned} \tag{7}$$

From Figs. 1 & 2, we note that thresholding a *single* snap can trigger several IEAs as a snap is essentially a temporal burst that spans a certain duration. Therefore, if τ is small, say $\tau \in [0, \Delta)$, then $R(\tau)$ is non-zero primarily due to IEAs triggered within the *same* DA or SR. Thus, Δ is the *effective length* of a thresholded snap. Consequently, we have from (7),

$$R(\tau) \approx p^2 + p\mathrm{P}[X(\tau) = \ell_1 | X(0) = \ell_1] \tag{8}$$

for $\tau \in [0, \Delta)$. Denoting the depth of a hydrophone by d (measured in meters) and assuming that snapping shrimp dwell at depths greater than d, we note that the maximum delay between a DA-SR pair is $2d/c$ ms, where c is the speed of sound (measured in km/s). This occurs if a snap originates directly beneath the hydrophone. Taking Δ into account, we observe that for the regime $\tau \in [\Delta, 2d/c + \Delta)$, the primary component of $R(\tau)$ is due to the dependency *between* arrivals in a DA-SR pair. This results in

$$R(\tau) \approx p^2 + \frac{p}{2}\mathrm{P}[X(t+\tau) = \ell_2 | X(t) = \ell_1] \tag{9}$$

for $\tau \in [\Delta, 2d/c + \Delta)$. Consequently, (7) can be approximated by the piecewise form

$$R(\tau) \approx \begin{cases} p^2 + p\mathrm{P}[X(\tau) = \ell_1 | X(0) = \ell_1] \\ \qquad\qquad \text{for } \tau \in [0, \Delta) \\ p^2 + \frac{p}{2}\mathrm{P}[X(\tau) = \ell_2 | X(0) = \ell_1] \\ \qquad\qquad \text{for } \tau \in [\Delta, 2d/c + \Delta) \\ p^2 \qquad\qquad \text{otherwise.} \end{cases} \tag{10}$$

The probabilities in (10) can be expressed in terms of the snap waveform and spatial density. This is done next.

Let $g(t)$ be a realization of a snap waveform and

$$h(t) = \begin{cases} 1 & \text{if } |g(t)| \geq \epsilon \\ 0 & \text{otherwise,} \end{cases} \tag{11}$$

where $h(0) = 1$ corresponds to the *first* IEA within the waveform $g(t)$. We denote $H(t)$ as the random process whose realization is $h(t)$ and note that $\mathrm{P}[H(t) = 0] = 1$ for $t < 0$ and $\mathrm{P}[H(0) = 1] = 1$. As $H(t)$ is effectively non-zero in the interval $t \in [0, \Delta)$, we have

$$\begin{aligned} &\mathrm{P}[X(\tau) = \ell_1 | X(0) = \ell_1] \\ &\qquad = \int_0^{\Delta} \mathrm{P}(H(\mu) = 1 | H(\mu - \tau) = 1) f(\mu) \mathrm{d}\mu, \end{aligned} \tag{12}$$

where $f(\mu) = 1/\Delta$ is the (uniform) probability density function (PDF) of observing $\mu \in [0, \Delta)$. For the same snap to be present at both $t = 0$ and $t = \tau$, the constraint $\mu \in [\tau, \Delta]$ needs to be enforced. This results in,

$$\mathrm{P}[X(\tau) = \ell_1 | X(0) = \ell_1] = p_H(\tau)/\Delta \quad \text{for } \tau \in [0, \Delta). \tag{13}$$

where

$$p_H(\tau) = \int_{\tau}^{\Delta} \mathrm{P}(H(\mu) = 1 | H(\mu - \tau) = 1) \mathrm{d}\mu. \tag{14}$$

Note that $p_H(\tau)$ is non-zero only within $\tau \in [0, \Delta)$. Moreover, as $X(\tau)$ is WSS, we have from Bayes' rule [16]

$$\mathrm{P}[X(\tau) = \ell_1 | X(0) = \ell_1] = \mathrm{P}[X(0) = \ell_1 | X(\tau) = \ell_1].$$

This allows the alternative form

$$p_H(\tau) = \int_0^{\Delta - \tau} \mathrm{P}(H(\mu) = 1 | H(\mu + \tau) = 1) \mathrm{d}\mu. \tag{15}$$

For the second probability term in (10), we have from the law of total probability,

$$\begin{aligned} &\mathrm{P}[X(\tau) = \ell_2 | X(0) = \ell_1] \\ &\qquad = \int_0^{\infty} \mathrm{P}[X(\tau) = \ell_2, R = r | X(0) = \ell_1] \mathrm{d}r, \end{aligned} \tag{16}$$

where r highlights the horizontal range from the hydrophone to the location of a snap that triggers the events $X(0) = \ell_1$ and $X(\tau) = \ell_2$. As the snap's spatial position is independent of $X(0) = \ell_1$, we have

$$\begin{aligned} &\mathrm{P}[X(\tau) = \ell_2 | X(0) = \ell_1] \\ &= \int_0^{\infty} \mathrm{P}[X(\tau) = \ell_2 | R = r, X(0) = \ell_1] \mathrm{P}[R = r] \mathrm{d}r. \end{aligned} \tag{17}$$

If h is the vertical distance (in meters) from the sensor to the sea floor, then the delay between a DA-SR pair is given by

$$\zeta(r) = \frac{\sqrt{r^2 + (2d + h)^2} - \sqrt{r^2 + h^2}}{c} \tag{18}$$

and is measured in milliseconds. Analogous to the approach used in deriving (12), we can express $\mathrm{P}[X(\tau) = \ell_2 | R = r, X(0) = \ell_1]$ in (17) in terms of $p_H(\tau)$. The derivation is cumbersome but requires the same insights and the use of both forms of $p_H(\tau)$ as highlighted in (14) and (15). The end results are

$$\begin{aligned} &\mathrm{P}[X(\tau) = \ell_2 | R = r, X(0) = \ell_1] \\ &= \begin{cases} \frac{p_H(|\tau - \zeta(r)|)}{\min(\zeta(r), \Delta)} & \text{for } \tau \in [\Delta, 2\Delta) \\ p_H(|\tau - \zeta(r)|)/\Delta & \text{for } \tau \in [2\Delta, 2d/c + \Delta) \\ 0 & \text{otherwise.} \end{cases} \end{aligned} \tag{19}$$

We note that (19) can incorporate general bathymetry by defining h to be the vertical distance of a snap from the hydrophone receiver. In our case, (18) implies that snaps originate from a flat seabed. Before (19) can be substituted into (17), we note that the integration interval in the latter needs to be constrained to ensure that $X(0) = \ell_1$ and $X(\tau) = \ell_2$ take place simultaneously. Thus, for a given τ, only snaps that occur within a certain range contribute to $R(\tau)$. This results in the piecewise function

$$\begin{aligned} &\mathrm{P}[X(\tau) = \ell_2 | X(0) = \ell_1] \\ &= \begin{cases} \int_{\zeta^{-1}(\tau + \Delta)}^{\zeta^{-1}(\tau - \Delta)} \frac{p_H(|\tau - \zeta(r)|)}{\min(\zeta(r), \Delta)} \mathrm{P}[R = r] \mathrm{d}r \\ \qquad \text{for } \tau \in [\Delta, 2\Delta) \\ \frac{1}{\Delta} \int_{\zeta^{-1}(\tau + \Delta)}^{\zeta^{-1}(\tau - \Delta)} p_H(|\tau - \zeta(r)|) \mathrm{P}[R = r] \mathrm{d}r \\ \qquad \text{for } \tau \in [2\Delta, 2d/c - \Delta) \\ \frac{1}{\Delta} \int_{\zeta^{-1}(2d/c)}^{\zeta^{-1}(\tau - \Delta)} p_H(|\tau - \zeta(r)|) \mathrm{P}[R = r] \mathrm{d}r \\ \qquad \text{for } \tau \in [2d/c - \Delta, 2d/c + \Delta) \\ 0 \qquad \text{otherwise.} \end{cases} \end{aligned} \tag{20}$$

On substituting (13) and (20) in (10), we finally get

$$R(\tau) \approx \begin{cases} p(p + p_H(\tau)/\Delta) & \text{for } \tau \in [0, \Delta) \\ p^2 + \frac{p}{2} \int_{\zeta^{-1}(\tau + \Delta)}^{\zeta^{-1}(\tau - \Delta)} \frac{p_H(|\tau - \zeta(r)|)}{\min(\zeta(r), \Delta)} \mathrm{P}[R = r] \mathrm{d}r \\ \qquad \text{for } \tau \in [\Delta, 2\Delta) \\ p^2 + \frac{p}{2\Delta} \int_{\zeta^{-1}(\tau + \Delta)}^{\zeta^{-1}(\tau - \Delta)} p_H(|\tau - \zeta(r)|) \mathrm{P}[R = r] \mathrm{d}r \\ \qquad \text{for } \tau \in [2\Delta, 2d/c - \Delta) \\ p^2 + \frac{p}{2\Delta} \int_{\zeta^{-1}(2d/c)}^{\zeta^{-1}(\tau - \Delta)} p_H(|\tau - \zeta(r)|) \mathrm{P}[R = r] \mathrm{d}r \\ \qquad \text{for } \tau \in [2d/c - \Delta, 2d/c + \Delta) \\ p^2 \qquad \text{otherwise.} \end{cases} \tag{21}$$

From (21), we note that $R(\tau)$ is parameterized by p, Δ, d, $p_H(\tau)$ and $\mathrm{P}[R = r]$. This sets up the forward model which we shall invert next.

IV. The Inverse Problem

On comparing the final mathematical form of $R(\tau)$ to the ACFs in Fig. 3, we clearly see the similarities between them. In fact, the interval $\tau \in [0, \Delta)$ corresponds to the regime before the neck, $\tau \in [\Delta, 2d/c - \Delta)$ between the neck and

shoulder and $\tau \in [2d/c-\Delta, 2d/c+\Delta)$ the regime between the shoulder and elbow. Consequently, Δ and d can be evaluated by detecting the 'bends' (maximum unsigned curvature) in the curves. This may be accomplished by employing a suitable one-dimensional edge detection technique such as the triangle method [17]. Note that Δ corresponds to the neck while $2d/c$ is the middle point between the shoulder and elbow. With obvious notation, for sensors 1 and 2, $\hat{d}$ was evaluated to be 1.86 m and 2.59 m, respectively, while $\hat{\Delta} = 0.41$ ms in either case. The estimated values of d were in line with the actual depth of the sensors.

With $\hat{d}$ and $\hat{\Delta}$ now evaluated, $p_H(\tau)$ can be estimated directly from (10) and (13). This results in

$$\hat{p}_H(\tau) = (\hat{R}(\tau)/\hat{p} - \hat{p})\hat{\Delta} \quad \text{for } \tau \in [0, \Delta), \tag{22}$$

where $\hat{p} = \hat{R}(0)$. Finding $\mathrm{P}[R = r]$ is not as straightforward as the integrals in (21) need to be discretized. This is further augmented by the fact that $\zeta(r)$ (and thus $\zeta^{-1}(\tau)$) are non-linear functions. However, by invoking a suitable sampling methodology, the estimation problem can be expressed as a linear program with linear constraints.

From (2), we note that $\hat{R}(\tau)$ is resolved at integer multiples of $1/f_s$. Our approach includes resolving Δ and $2d/c$ to the nearest integer multiple of $1/f_s$. More precisely, let $\Delta = M/f_s$ and $2d/c = L/f_s$, where $M, L \in \mathbb{Z}^+$. Furthermore, we set a maximum horizontal distance $r_{\max} = \zeta^{-1}(\tau_{\min})$ for snaps that trigger IEAs at the hydrophone receiver, where $\tau_{\min} = V/f_s$ is the minimum possible delay between a DA-SR pair for some $V \in \mathbb{Z}^+$. We consider the scenario where $L \geq 2M$ and $M \geq V$ are satisfied. Also, $\mathrm{P}[R = r]$ only influences $R(\tau)$ within the interval $\tau \in [\Delta, 2d/c + \Delta)$, which after discretization includes the samples $\tau = k/f_s \ \forall \ k \in \{M, M+1, \ldots, L+M-1\}$. We also define

$$\begin{aligned} r_i &= \zeta^{-1}(2d/c - (i-1)/f_s) = \zeta^{-1}((L-i+1)/f_s), \\ &\triangleq \zeta^{-1}[L-i+1], \end{aligned} \tag{23}$$

for $i \in \{1, 2, \ldots, L-V\}$. On combining the aforementioned characteristics, we have from (21)

$$\begin{aligned} &\frac{2}{p}(R[k] - p^2) \\ &= \begin{cases} \sum_{i=L-M-k+1}^{\min(L-V, L+M-k)} \frac{p_H[|k-L+i-1|]}{\min(\zeta(r_i), \Delta)} \mathrm{P}[r_i \leq R < r_{i+1}] \\ \qquad \text{for } k \in \{M, \ldots, 2M-1\} \\ \frac{1}{\Delta} \sum_{i=L-M-k+1}^{L+M-k} p_H[|k-L+i-1|] \mathrm{P}[r_i \leq R < r_{i+1}] \\ \qquad \text{for } k \in \{2M, \ldots, L-M-1\} \\ \frac{1}{\Delta} \sum_{i=1}^{L+M-k} p_H[|k-L+i-1|] \mathrm{P}[r_i \leq R < r_{i+1}] \\ \qquad \text{for } k \in \{L-M, \ldots, L+M-1\}. \end{cases} \end{aligned}$$

Let $\mathbf{q} = [q_1, q_2, \ldots, q_{L-V-1}]^\mathsf{T}$, where $q_i = \mathrm{P}[r_i \leq R < r_{i+1}]$. We also define the vector $\hat{\mathbf{y}} = [y_1, y_2, \ldots, y_L]^\mathsf{T}$, where

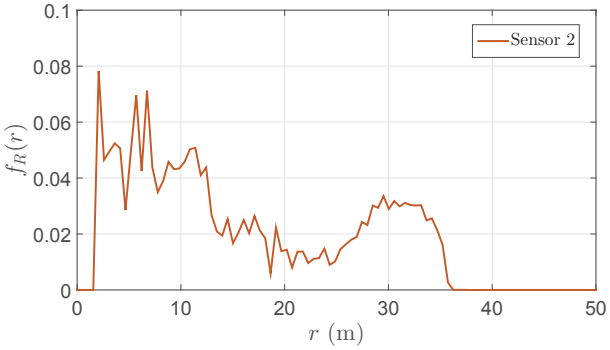

Fig. 5. The spatial snap distribution evaluated from sensor 2.

$\hat{y}_j = \frac{2}{\hat{p}}(\hat{R}[L+M-j] - \hat{p}^2)$. To enable the inversion, we adopt the constrained least squares framework,

$$\begin{aligned} \hat{\mathbf{q}} \ = \ \underset{\boldsymbol{\mu}}{\mathtt{argmin}} \quad & \|\hat{\mathbf{y}} - \hat{\mathbf{A}}\boldsymbol{\mu}\| \\ \mathtt{s.t} \quad & \boldsymbol{\mu} \geq 0 \\ & \|\boldsymbol{\mu}\|_1 \leq 1, \end{aligned} \tag{24}$$

where $\|\cdot\|_1$ denotes the L_1-norm, $\boldsymbol{\mu} \geq 0$ implies that all elements of $\boldsymbol{\mu}$ are greater than zero and $\hat{\mathbf{A}} \in \mathbb{R}^{L \times (L-V-1)}$ is a tall banded matrix which can be constructed completely from $\hat{p}_H[k]/\min(\zeta(r_i), \Delta) \ \forall \ k \in \{0, 1, \ldots, M-1\}$. The constraints in (24) guarantee q_i to be probabilities of non-overlapping intervals in R. Do note that $\|\boldsymbol{\mu}\|_1 \leq 1$ is deliberately set as an equality to allow for model mismatch, as snaps beyond $r_{\max}$ may possibly trigger IEAs at the hydrophone receiver. Finally, as $r_{i+1} - r_i$ is non-uniform in i, we compute

$$f_R(r_i) = q_i/(r_{i+1} - r_i), \tag{25}$$

which is the estimated PDF of observing a snap at $R = r$ and interpolate it at uniform sampling intervals. This is plotted for sensor 2 in Fig. 5 for a range resolution of 0.5 m.

V. Conclusion

We explored the possibility of extracting environmental information from noise samples recorded by a single hydrophone receiver in warm shallow waters. By working with IEAs rather than noise observations, we essentially bypassed the amplitude statistics and considered only the temporal component within. The corresponding ACFs exhibited a certain structure. A two-ray model consisting of DAs and SRs was subsequently derived that was able to model the transitions within the data ACF. The model was parameterized by the effective snap length, receiver depth and spatial distribution of the snaps. Methods to solve the inverse problem were also proposed. Our results highlight the potential of determining spatial snap distributions with a minimalistic setup. This may offer significant advantages in the realm of underwater environmental monitoring. Moreover, the snap distribution and approach adopted in this work may be used in the development of spatial noise models for hydrophone arrays.

ACKNOWLEDGEMENTS

The authors extend their gratitude to Koay Teong Beng of the Acoustic Research Laboratory (ARL) at the National University of Singapore (NUS), who recorded and provided the ambient noise data considered in this work.

REFERENCES

[1] M. W. Legg, "Non-Gaussian and non-homogeneous Poisson models of snapping shrimp noise," Ph.D. dissertation, Curtin Univ. of Technology, 2009.

[2] M. Chitre, M. Legg, and T.-B. Koay, *Snapping shrimp dominated natural soundscape in Singapore waters*, ser. Contributions to Marine Sci. Nat. Univ. of Singapore, 2012.

[3] M. Chitre, S. Kuselan, and V. Pallayil, "Ambient noise imaging in warm shallow waters; robust statistical algorithms and range estimation," *The J. of the Acoustical Soc. of Amer.*, vol. 132, no. 2, 2012.

[4] A. Mahmood and M. Chitre, "Temporal analysis of stationary Markov α-sub-Gaussian noise," in *MTS/IEEE Oceans - Monterey, 2016*, Sep 2016, pp. 1–6.

[5] J. R. Potter, T. W. Lim, and M. A. Chitre, "Ambient noise environments in shallow tropical seas and the implications for acoustic sensing," *Oceanology Int.*, vol. 97, pp. 2114–2117, 1997.

[6] A. Mahmood and M. Chitre, "Modeling colored impulsive noise by Markov chains and alpha-stable processes," in *MTS/IEEE Oceans - Genoa, 2015*, May 2015, pp. 1–7.

[7] K. T. Beng, T. E. Teck, M. Chitre, and J. Potter, "Estimating the spatial and temporal distribution of snapping shrimp using a portable, broadband 3-dimensional acoustic array," in *MTS/IEEE Oceans - San Diego, 2003*, vol. 5, Sept 2003, pp. 2706–2713 Vol.5.

[8] S. D. Simpson, M. Meekan, J. Montgomery, R. McCauley, and A. Jeffs, "Homeward sound," *Science*, vol. 308, no. 5719, pp. 221–221, 2005.

[9] A. Mahmood and M. Chitre, "Optimal and near-optimal detection in bursty impulsive noise," *IEEE J. Ocean. Eng.*, vol. PP, no. 99, pp. 1–15, 2016.

[10] A. Mahmood, H. Vishnu, and M. Chitre, "Model-based signal detection in snapping shrimp noise," in *2016 IEEE Third Underwater Commun. and Networking Conf. (UComms)*, Aug 2016, pp. 1–5.

[11] T. Y. Min, M. Chitre, and V. Pallayil, "Detecting the direction of arrival and time of arrival of impulsive transient signals," in *OCEANS 2016 MTS/IEEE Monterey*, Sept 2016, pp. 1–8.

[12] ——, "Detecting the direction of arrival and time of arrival of impulsive transient signals," in *OCEANS 2016 MTS/IEEE Monterey*, Sept 2016, pp. 1–8.

[13] J. Nolan, "Maximum likelihood estimation and diagnostics for stable distributions," in *Lévy Processes*, O. Barndorff-Nielsen, S. Resnick, and T. Mikosch, Eds. Birkhuser Boston, 2001, pp. 379–400. [Online]. Available: http://dx.doi.org/10.1007/978-1-4612-0197-7_17

[14] G. Samorodnitsky and M. S. Taqqu, *Stable Non-Gaussian Random Processes: Stochastic Models with Infinite Variance*. Chapman & Hall, 1994.

[15] J. P. Nolan, *Stable Distributions - Models for Heavy Tailed Data*. Boston: Birkhauser, 2015, in progress, Chapter 1 online at. [Online]. Available: http://fs2.american.edu/jpnolan/www/stable/stable.html

[16] A. Papoulis and U. S. Pillai, *Probability, Random Variables and Stochastic Processes*. Boston: McGraw-Hill, Dec 2001.

[17] G. W. Zack, W. E. Rogers, and S. A. Latt, "Automatic measurement of sister chromatid exchange frequency," *J. of Histochemistry & Cytochemistry*, vol. 25, no. 7, pp. 741–753, 1977.